THE JOURNAL OF PHYSICAL CHEMISTRY B

Article

pubs.acs.org/JPCB

Miscibility and Thermodynamics of Mixing of Different Models of Formamide and Water in Computer Simulation

Bálint Kiss,[†,‡] Balázs Fábián,[§,∥] Abdenacer Idrissi,[‡] Milán Szőri,[†] and Pál Jedlovszky*[,⊥]

[†]Institute of Chemistry, University of Miskolc, Egyetemváros A/2, H-3515 Miskolc, Hungary

[‡]Laboratoire de Spectrochimie Infrarouge et Raman (UMR CNRS 8516), University of Lille Nord de France, 59655 Villeneuve d'Ascq Cedex, France

[§]Department of Inorganic and Analytical Chemistry, Budapest University of Technology and Economics, Szt. Gellért tér 4, H-1111 Budapest, Hungary

[∥]Institut UTINAM (CNRS UMR 6213), Université Bourgogne Franche-Comté, 16 route de Gray, F-25030 Besançon, France

[⊥]Department of Chemistry, Eszterházy Károly University, Leányka utca 6, H-3300 Eger, Hungary

ABSTRACT: The thermodynamic changes that occur upon mixing five models of formamide and three models of water, including the miscibility of these model combinations itself, is studied by performing Monte Carlo computer simulations using an appropriately chosen thermodynamic cycle and the method of thermodynamic integration. The results show that the mixing of these two components is close to the ideal mixing, as both the energy and entropy of mixing turn out to be rather close to the ideal term in the entire composition range. Concerning the energy of mixing, the OPLS/AA_mod model of formamide behaves in a qualitatively different way than the other models considered. Thus, this model results in negative, while the other ones in positive energy of mixing values in combination with all three water models considered. Experimental data supports this latter behavior. Although the Helmholtz free energy of mixing always turns out to be negative in the entire composition range, the majority of the model combinations tested either show limited miscibility, or, at least, approach the miscibility limit very closely in certain compositions. Concerning both the miscibility and the energy of mixing of these model combinations, we recommend the use of the combination of the CHARMM formamide and TIP4P water models in simulations of water−formamide mixtures.

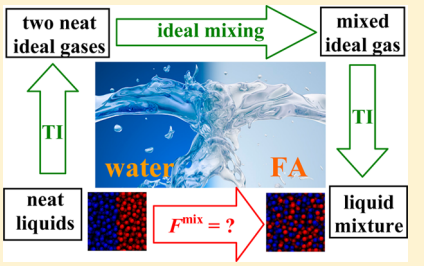

INTRODUCTION

Liquid formamide (H−CO-NH_2) and its aqueous mixtures are systems of great importance, both from the purely scientific, theoretical point of view and also from that of industrial applications. Formamide is a highly polar, hygroscopic liquid of unusually high dielectric constant, which is fully miscible with water.[1] The high dielectric constant of formamide of about 109[2] cannot simply be explained by the large molecular dipole moment of 3.7 D.[3] Thus, for instance, the dielectric constant of its double methylated derivative, *N*,*N*-dimethylformamide, is only 37,[2] despite the fact that the dipole moment of this molecule is as large as 3.9 D.[3] Instead, the large dielectric constant of liquid formamide is related to the fact that its molecules exhibit extensive hydrogen bonding, involving both N−H- and C−H-donated hydrogen bonds. In fact, similarly to water,[4,5] formamide is also a network forming liquid,[6,7] and hence these molecules can locally substitute each other in the hydrogen bond network,[8] although such substitution may change the topology of the network.[7,9] Due to this, and other similar properties of the two liquids, mixtures of formamide and water are thought to be prototypes of the ideal mixture.[10,11] Consistently, the energy and enthalpy change occurring upon mixing the two compounds in any proportion turned out to be a very small, positive value, both experimentally[12,13] and in computer simulation.[14]

Industrial importance of formamide and its aqueous mixtures is due to their high dielectric constant, which makes these systems very good solvents of many heavy metal salts as well as of salts of alkali and alkaline-earth metals.[15] Further, formamide is an important solvent for resins, and it is also used as a softener for paper, in animal glues, and water-soluble gums. Mixtures of formamide and water are excellent plasticizers for thermoplastic starch polylactic acid blends.[16] As a chemical intermediate, formamide is particularly useful in the synthesis of heterocyclic compounds, pharmaceutical (e.g., vitamins), crop protection agent, pesticides, and for the manufacture of hydrocyanic acid.[1] Formamide may be released into the environment during its manufacturing process, and the fate of atmospheric formamide is mainly due to its rainout.[17]

From the scientific point of view, the importance of formamide stems from the fact that it is the smallest molecule that contains a peptide bond, and also the simplest molecule that is able to form N−H···O type hydrogen bonds. Thus,

Received: May 23, 2017
Revised: June 27, 2017
Published: June 28, 2017

DOI: 10.1021/acs.jpcb.7b04965
J. Phys. Chem. B XXXX, XXX, XXX−XXX

aqueous mixtures of formamide are often considered as model systems in studying various properties of hydrated proteins and polypeptides, e.g., how hydrogen bonds[18,19] and peptide bonds[20] are formed and broken, or how water exercises kinetic and thermodynamic control over the chemical activities of polypeptides.[21] These mixtures can also be used as reference systems to study hydrophobic and hydrophilic interactions.[22] Further, aqueous formamide solutions are thought to play a non-negligible role in prebiotic evolution. Clearly, there is an increasing body of both theoretical and experimental evidence suggesting that formamide is a potential hub in the complex network of prebiotic chemical reactions that leads from simple precursors, such as H_2, H_2O, N_2, NH_3, CO, and CO_2, to key biological molecules.[23−25]

Due to the aforementioned reasons, both neat liquid formamide[6,7,20,22,26−29] and its aqueous mixtures[8,10,11,14,19,30−33] have been studied by computer simulation methods several times. However, in simulating liquid mixtures one has to face the problem that potential models that work perfectly for the respective neat liquids might be incompatible with each other, resulting in a poor reproduction of the properties of the mixtures. If the thermodynamic driving force behind the miscibility of the two compounds is small, this might even involve limited miscibility of certain models of the two fully miscible compounds.[34,35] Since the mixing of water and formamide is close to the ideal mixing,[10−14] the thermodynamic changes occurring upon their mixing are expected to be rather small (as it was already shown concerning their energy of mixing.[12−14]) As a consequence, the thermodynamic driving force of this mixing must be small, which makes the above issue, concerning the compatibility of the potential models with each other and their ability to reproduce full miscibility, particularly important for mixtures of water and formamide.

In this article, we study the thermodynamics of mixing formamide and water by computer simulation, concerning five widely used formamide and three such water models. Besides calculating the Helmholtz free energy, energy, and entropy of mixing of these model combinations in the entire composition range, we also analyze which of these model pairs are fully miscible with each other, and which of them exhibit miscibility gaps. Thermodynamic changes occurring upon mixing are calculated along an appropriately chosen thermodynamic cycle[36] using the method of thermodynamic integration.[37,38] This approach has already successfully been used to study the thermodynamics of mixing of various pairs of fluids.[34−36,39−41] The performance of the different model combinations considered are evaluated (i) according to their ability to reproduce full miscibility, and (ii) by comparing the calculated energy of mixing to existing experimental data.[12,13]

The rest of the article is organized as follows. In the Methods Section the applied methods, including the thermodynamic path used and the method of thermodynamic integration, are explained in detail. The simulations performed and potential models considered in this study are also described here. The obtained results are presented and discussed in detail in the Results and Discusion Section. Finally, in the Summary and Conclusions Section the main conclusions of this work are summarized.

METHODS

Thermodynamics of Mixing. The thermodynamic condition that two liquid compounds, A and B, are fully miscible with each other can be formulated as the inequality[42]

$$D = 1 + x_A x_B \frac{\partial^2 (F^{ex}/RT)}{\partial^2 x_A} > 0 \quad (1)$$

holds in the entire composition range of $0 < x_A < 1$. Here, x_A and x_B denote the mole fraction of the respective components, R is the gas constant, T is the temperature, and F^{ex} is the excess molar Helmholtz free energy with respect to the ideal mixing of the two components:

$$F^{ex} = F^{mix} - RT(x_A \ln x_A + x_B \ln x_B) \quad (2)$$

In this equation, F^{mix} denotes the total Helmholtz free energy change accompanying the mixing of the neat components A and B (often simply called as their free energy of mixing).

F^{mix} can be calculated by considering the following thermodynamic cycle (see Figure 1).[36] In the first step, the neat components are brought from the liquid to the ideal gas state under isochoric conditions. In the second step, the two components are mixed in the ideal gas state; this step is accompanied by the free energy change of the ideal mixing of $RT(x_A \ln x_A + x_B \ln x_B)$. Finally, in the third step, the mixture is brought back isochorically from the ideal gas to the liquid state. Thus, the free energy change of the net process, F^{mix}, can be written as

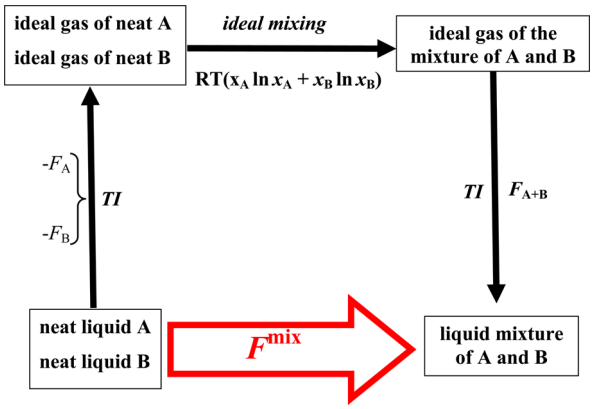

Figure 1. Schematic diagram showing the thermodynamic cycle along which the free energy of mixing of the two components is calculated. For a detailed explanation, see the text.

$$F^{mix} = F_{A+B} - x_A F_A - x_B F_B + RT(x_A \ln x_A + x_B \ln x_B) \quad (3)$$

where F_A, F_B, and F_{A+B} are the Helmholtz free energies of the corresponding systems (i.e., neat liquid A, neat liquid B, and their mixture, respectively) with respect to their ideal gas state. It should be noted that the inequality $F^{mix} < 0$ is not a sufficient condition of miscibility, as it simply reflects that the mixture is thermodynamically more stable than the two separate neat components. However, miscibility also requires that the single phase mixture is stable also with respect to any two phase systems consisting of mixed phases of different compositions. This condition is taken into account in eq 1.

Using the same thermodynamic cycle as for the calculation of F^{mix}, and considering that mixing in the ideal gas state is

DOI: 10.1021/acs.jpcb.7b04965
J. Phys. Chem. B XXXX, XXX, XXX−XXX

accompanied by no energy change, the energy of mixing of the two components, U^{mix}, can be written as

$$U^{mix} = U_{A+B} - x_A U_A - x_B U_B \quad (4)$$

where U_A, U_B, and U_{A+B} denote the internal energies of the corresponding systems. Finally, the entropy of mixing of the two components, S^{mix}, can simply be calculated from U^{mix} and F^{mix} as

$$S^{mix} = \frac{U^{mix} - F^{mix}}{T} \quad (5)$$

Thermodynamic Integration. While the terms U_A, U_B, and U_{A+B} in eq 4 can simply be calculated in computer simulation as the total potential energy of the corresponding systems, the determination of F_A, F_B, and F_{A+B} in eq 3 is not that straightforward. In general, the configurational part of the Helmholtz free energy, being proportional to the logarithm of the configurational integral (i.e., configurational part of the total partition function) on the canonical ensemble, is far more difficult to be accessed in a computer simulation than other thermodynamic quantities, such as the internal energy. This is because here the entire configurational space needs to be sampled instead of only its lowest energy domains. (The kinetic part of the Helmholtz free energy depends only on the velocities of the particles, and hence remains unchanged at constant temperature.) It can be computationally feasible, however, to calculate the free energy difference between two states, as in this case only those domains of the configurational space are needed to be sampled that are considerably different in the two states.

In the method of thermodynamic integration (TI),[37,38] the difference of the Helmholtz free energies between states X and Y is calculated as an integral along an arbitrarily chosen path connecting the two states:

$$\Delta F = F_Y - F_X = \int_0^1 \left(\frac{\partial F(\lambda)}{\partial \lambda}\right) d\lambda \quad (6)$$

where λ is the coupling parameter that describes this path, its value being 0 in state X and 1 in state Y. Considering the fundamental relations of statistical mechanics that $F = -k_B T \ln Q$ and $Q = \int \exp(-U/k_B T) d\mathbf{q}^N$, the integrand of eq 6 can be written as

$$\frac{\partial F(\lambda)}{\partial \lambda} = -k_B T \frac{1}{Q(\lambda)} \frac{\partial Q(\lambda)}{\partial \lambda} = \frac{\int \frac{\partial U(\lambda)}{\partial \lambda} \exp(-\beta U(\lambda)) d\mathbf{q}^N}{\int \exp(-\beta U(\lambda)) d\mathbf{q}^N} = \left\langle \frac{\partial U(\lambda)}{\partial \lambda} \right\rangle_\lambda \quad (7)$$

where Q is the configurational integral, $\mathbf{q}^N$, which denotes the coordinates of all N particles in the system, represents a given point of the configurational space, k_B is the Boltzmann constant, $\beta = 1/k_B T$, and the brackets $\langle \cdots \rangle_\lambda$ denote ensemble averaging at the state corresponding to the given value of λ.

When connecting states X and Y, a polynomial path is usually chosen. Considering also that in systems where the energy is pairwise additive, and the leading term of the pair potential (i.e., steric repulsion) decays with r^{-12}, this polynomial has to be at least of fourth order to avoid divergence of $U(\lambda)$ at $\lambda = 0$,[37] this path is conventionally chosen in computer simulations as

$$U(\lambda) = \lambda^4 U_Y + (1 - \lambda)^4 U_X \quad (8)$$

where U_X and U_Y are the energies of the corresponding states. If the Helmholtz free energy difference between the (isochoric) liquid and ideal gas states of a system needs to be calculated,[43−47] as in the present case, eq 8 can be simplified to $U(\lambda) = \lambda^4 U_Y$, considering that the potential energy in the ideal gas state, X, is zero. In this case, using also eq 7, eq 6 can be rewritten as

$$\Delta F = \int_0^1 \left\langle \frac{\partial U(\lambda)}{\partial \lambda} \right\rangle_\lambda d\lambda = \int_0^1 4\lambda^3 \langle U_Y \rangle_\lambda d\lambda \quad (9)$$

Further, the Boltzmann factor in eq 7, evaluated in each step of a Monte Carlo simulation, can be rewritten as

$$\exp(-U(\lambda)/k_B T) = \exp(-\lambda^4 U_Y/k_B T) = \exp(-U_Y/k_B (T/\lambda^4)) = \exp(-U_Y/k_B T^*) \quad (10)$$

where $T^* = T/\lambda^4$. Therefore, a simulation performed at a given λ point along the (fictitious) path connecting states X and Y with the potential function $U(\lambda)$, needed to evaluate the ensemble average in eq 7, can be substituted with a simulation performed in state Y (i.e., at $\lambda = 1$, in the liquid state of interest) with the full potential function $U(1) = U_Y$, but at the virtual temperature $T^* = T/\lambda^4$. In other words, the path connecting the liquid and ideal gas states along λ by gradually decreasing the potential energy to zero can be substituted by a path along which the temperature of the system is increased gradually to infinity. This way, the ideal gas state is simply defined as a state of infinite kinetic energy rather than that of zero potential energy. It should be recalled that the path connecting states X and Y is fictitious, therefore, the points along which it passes (i.e., the systems simulated at various virtual temperatures T^*) have no physical relevance by themselves. These fictitious states only serve to connect the two end points of the path, i.e., the two states that are of real physical relevance, the free energy difference of which is to be calculated. Having the ensemble average of eq 7 thus evaluated at several values of λ (or T^*), the integral of eq 9 can be performed, and ΔF can be calculated.

The values of F_A, F_B, and F_{A+B} in eq 3 have been calculated using the above-described method of thermodynamic integration. Monte Carlo simulations have been performed at six different (virtual) temperatures, corresponding to the λ values of 0.046911, 0.230765, 0.5, 0.769235, 0.953089, and 1. The first five λ values correspond to the 5-point Gaussian quadrature,[48] while simulations at the nonfictitious state $\lambda = 1$ have been performed in order to also evaluate U_A, U_B, and U_{A+B}. To perform the integral of eq 9, a fourth order polynomial has been fitted to the $4\lambda^3 \langle U_Y \rangle_\lambda$ vs λ data points, and the fitted polynomial has been integrated analytically. These points, along with the fitted polynomial, are shown in Figure 2, as obtained in selected systems.

Monte Carlo Simulations. The integrand of eq 9 has been evaluated by performing a Monte Carlo simulation at each λ value considered for each system. The real temperature of the systems, corresponding to $\lambda = 1$ has been 298 K. In every simulation, 512 molecules have been placed in a cubic basic simulation box, the edge length of which, L, has been set in order to reproduce the experimental mass density[49] of the system (see Table 1). Besides the two neat systems, mixtures of nine different compositions, corresponding to the formaldehyde mole fraction (x_{FA}) values of 0.1, 0.2, 0.3, 0.4, 0.5,

DOI: 10.1021/acs.jpcb.7b04965
J. Phys. Chem. B XXXX, XXX, XXX−XXX

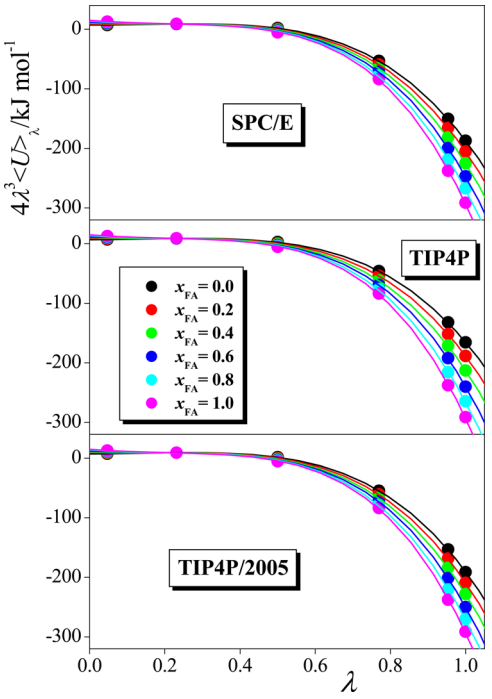

Figure 2. Integrand of the thermodynamic integration (eq 9), obtained at six λ points for the combination of the CHARMM model of formamide with the SPC/E (top panel), TIP4P (middle panel), and TIP4P/2005 (bottom panel) models of water (full circles), together with the fourth order polynomials fitted to these data (solid curves) at the formamide mole fraction values of 0 (black), 0.2 (red), 0.4 (green), 0.6 (dark blue), 0.8 (light blue), and 1.0 (magenta).

Table 1. Properties of the Systems Simulated

x_{FA}	N_{FA}	N_{wat}	ρ/g cm^{-3}	L/Å
0	0	512	0.997	24.85
0.1	51	461	1.028	25.81
0.2	102	410	1.051	26.69
0.3	154	358	1.068	27.52
0.4	205	307	1.082	28.32
0.5	256	256	1.093	29.08
0.6	307	205	1.103	29.80
0.7	358	154	1.111	30.49
0.8	410	102	1.118	31.15
0.9	461	51	1.124	31.78
1	512	0	1.130	32.39

0.6, 0.7, 0.8, and 0.9 have been simulated. The characteristics of the different systems simulated are collected in Table 1.

All simulations have been performed with the program MMC.[50] In a Monte Carlo step, a randomly chosen molecule has been randomly displaced to a maximum distance of 0.25 Å, and randomly rotated by no more than 10°. The geometry of all molecules has been kept unchanged in the simulations. At least 25% of the trial moves have been successful in every case. All interactions have been truncated to zero beyond the center−center cutoff distance of 12.4 Å, the O and N atoms being regarded as the centers of the water and formamide molecules, respectively. The long-range part of the electrostatic interaction has been accounted for using the reaction field correction method[51−53] under conducting boundary conditions. The systems have been equilibrated through 5×10^7 Monte Carlo steps; the value of $< U_Y >$ has then been evaluated in a consecutive, 10^8 Monte Carlo steps long equilibrium trajectory.

Potential Models. In the present study, we consider the mixing of five different models of formamide with three widely used water models. Since simulations have been performed at six (virtual) temperatures and nine compositions for each model combination and also for the neat systems, the total number of simulations performed is 858. The formamide potentials considered include the united atom OPLS model,[2] the OPLS/AA model[54] modified by Pérez de la Luz et al.[28] (referred to here as OPLS/AA_mod), the model belonging to the CHARMM force field,[55] and those proposed by Cordeiro[27] and by Macchiagodena et al.,[29] referred to here as MMPB. For water, we consider the three-site SPC/E[56] and four-site TIP4P[57] and TIP4P/2005[58] potentials. It should be noted that, without additional testing, the CHARMM force field is supposed to be used in combination with the SPC/E, while OPLS with the TIP4P water model. However, the present study represents a far more stringent test of the model combinations considered than the ones on which such "thumb rules" are based, hence all possible combinations of the above models are included in the following analyses.

All models considered are pairwise additive; the interaction energy of two molecules, i and j, being within the center−center cutoff distance, is calculated as

$$u_{ij} = \sum_{\alpha=1}^{N_i} \sum_{\beta=1}^{N_j} \frac{1}{4\pi\in_0} \frac{q_\alpha q_\beta}{r_{i\alpha,j\beta}} + 4\varepsilon_{\alpha\beta}\left[\left(\frac{\sigma_{\alpha\beta}}{r_{i\alpha,j\beta}}\right)^{12} - \left(\frac{\sigma_{\alpha\beta}}{r_{i\alpha,j\beta}}\right)^{6}\right] \quad (11)$$

Here indices α and β run over the N_i and N_j interaction sites of molecules i and j, respectively, $\in_0$ is the vacuum permittivity, $r_{i\alpha,j\beta}$ is the distance of site α on molecule i from site β on molecule j, q_α and q_β are the fractional charges corresponding to the respective interaction sites, while $\varepsilon_{\alpha\beta}$ and $\sigma_{\alpha\beta}$ are the energy and distance parameters, respectively, of the Lennard-Jones interaction of sites α and β, related to the corresponding parameters of the individual sites through the Lorentz−Berthelot rule,[53] i.e., $\varepsilon_{\alpha\beta} = (\varepsilon_\alpha\varepsilon_\beta)^{1/2}$ and $\sigma_{\alpha\beta} = (\sigma_\alpha+\sigma_\beta)/2$. We have repeated the simulations involving the OPLS or OPLS/AA_mod formamide models using also the geometric means of both Lennard-Jones parameters, but this change in the potential has left all of our conclusions unchanged.

In the water models considered, the O atom is the only center of a Lennard-Jones interaction, and the H atoms bear a fractional charge of q_H. The negative fractional charge compensating them is located on the O atom in the SPC/E model, but it is displaced from the O atom by r_{OM} to a

Table 2. Geometry and Interaction Parameters of the Water Models Used

model	reference	r_{OH}/Å	r_{OM}/Å	α_{HOH}/deg	σ/Å	ε/kJ mol^{-1}	q_H/e
SPC/E	56	1.000	0	109.47	3.1660	0.650	0.4238
TIP4P	57	0.9572	0.15000	104.52	3.1540	0.649	0.5200
TIP4P/2005	58	0.9572	0.1546	104.52	3.1589	0.775	0.5564

DOI: 10.1021/acs.jpcb.7b04965
J. Phys. Chem. B XXXX, XXX, XXX−XXX

nonatomic interaction site, M, along the bisector of the H−O−H bond angle, α_{HOH}, in the TIP4P and TIP4P/2005 models. The parameters of the water models considered are collected in Table 2. The OPLS model of formamide consists of only five interaction sites; the CH group is treated in this model as a united atom. The OPLS/AA_mod, CHARMM, and Cordeiro models have interaction sites on all six atoms, while in the MMPB model the fractional charge is displaced from the O atom to two nonatomic interaction sites, denoted as L, located at the distance of 0.31 Å from the O atom along its two lone pair directions. According to the molecular geometry of formamide, all interaction sites are arranged in a planar way in all of these models. The interaction parameters of the formamide models considered are collected in Table 3.

Table 3. Interaction Parameters of the Formamide Models Used

model	reference	site	σ/Å	ε/kJ mol^{-1}	q/e
OPLS	2	CH	3.80	0.4815	0.500
		O	2.96	0.8792	−0.500
		N	3.25	0.7118	−0.850
		H			0.425
OPLS/AA_mod	28	C	3.80625	0.307524	0.1398
		O	3.00440	0.615048	−0.5283
		H(C)	2.45630	0.043932	0.1753
		N	3.29875	0.497896	−0.4163
		H			0.3121[b]
					0.3174[c]
CHARMM	55	C	3.175	0.293	0.42
		O	2.700	0.502	−0.51
		H(C)	2.100	0.090	0.08
		N	2.940	0.837	−0.69
		H	0.356	0.192	0.35
Cordeiro	27	C	3.75	0.440	0.340
		O	2.96	0.880	−0.460
		H(C)	2.75	0.159	0.120
		N	3.25	0.712	−0.830
		H			0.415
MMPB	29	C	3.75	0.43932	0.154544
		O	2.96	0.87864	0
		L[a]			−0.201887
		H(C)	2.42	0.06276	0.131902
		N	3.25	0.71128	−0.566816
		H			0.339036[b]
					0.345109[c]

[a]Nonatomic interaction site. [b]H atom in cis relative position with the carboxylic oxygen. [c]H atom in trans relative position with the carboxylic oxygen.

RESULTS AND DISCUSSION

The Helmholtz free energy, energy, and entropy of the water−formamide mixtures of various compositions, including the two neat systems, with respect to the ideal gas state are shown in panels a, b, and c of Figure 3, respectively, as obtained from the thermodynamic integration for the various model combinations considered. These quantities show a nearly linear composition dependence in most cases, suggesting that the mixing of the two components is probably close to the ideal mixing. Markedly different behavior was previously seen for mixtures of acetone both with water[34,35] and methanol.[40] The free energy of the liquid decreases with increasing formamide mole fraction. This free energy decrease is clearly of energetic origin, as both the energy and the entropy of the systems decrease as the formamide concentration increases. It is also seen that these quantities can be rather different for different model combinations. This difference mainly originates from the different thermodynamic properties of the formamide models considered: the difference of the Helmholtz free energy, energy, and entropy of neat formamide can be as large as 50, 35, and 20%, respectively, when different potentials are considered.

The Helmholtz free energy, energy, and entropy change accompanying the mixing of neat liquid water and formamide are plotted in panels a, b, and c of Figure 4, respectively, as obtained with the different model combinations. As is clear from the figure, the free energy of mixing is negative in every case, indicating that the mixture is always thermodynamically more stable than the two separate neat liquids. The magnitude of F^{mix} is rather small, being always below 2 kJ/mol. For comparison, the value of RT is about 2.5 kJ/mol at 298 K. (The value of $RT/2$, i.e., the average kinetic energy of the molecules along one single degree of freedom, is shown for comparison in Figure 4.) Similarly, small values are obtained for U^{mix} and S^{mix} in every case, their values being always within $RT/2$ and $R/2$, respectively. As a consequence, the obtained F^{mix}, U^{mix}, and S^{mix} values are also rather close to each other as obtained with different model combinations, their difference never exceeds 1.3, 1.8, and 3.5 J/(mol K), respectively. The free energy of mixing is the smallest in magnitude as obtained with the OPLS, Cordeiro, and MMPB models of formamide (the results obtained with these three models are always within error bars of each other), and deepest as obtained with the OPLS/AA_mod model. No marked difference is seen between the water models in this respect.

The energy of mixing shows a qualitatively different behavior when the OPLS/AA_mod model of formamide is considered than what is seen with the other formamide models. Namely, it is always below zero in mixtures of the OPLS/AA_mod model, but it is positive in all other cases. Although the deviation from the experimental values[12,13] is roughly of the same magnitude with all formamide models considered, the experimental data supports the qualitative behavior of the OPLS, CHARMM, Cordeiro, and MMPB models rather than that of OPLS/AA_mod in this respect. Thus, according to the experimental data,[12,13] the observed negative free energy of mixing of water and formamide is of entropic origin, as the energy of mixing is very small and positive. Consistently, the entropy of mixing is found to be positive for all model combinations, being the largest when the CHARMM model of formamide is considered.

Figure 4c also includes the entropy change corresponding to ideal mixing, i.e., $-R\,[x_{FA}\ln x_{FA} + (1 - x_{FA})\ln(1 - x_{FA})]$. As is clearly seen from the figure, the obtained S^{mix} values are rather close to this ideal term; their difference never exceeds 2.5 J/(mol K), and, considering the OPLS, Cordeiro, and MMPB models, this difference always remains below 1 J/(mol K), being within the error bars of the calculation. The largest entropy of mixing values are always obtained with the CHARMM, while the smallest ones with the OPLS/AA_mod model of formamide, the $S^{mix}(x_{FA})$ curves obtained with the former model being always clearly above, and those with the latter one always below the values corresponding to the entropy of ideal mixing. Thus, contrary to the case of OPLS/AA_mod, the relatively low free energy of mixing values obtained with the CHARMM model of formamide are of entropic origin, while for the other three formamide models the obtained negative

DOI: 10.1021/acs.jpcb.7b04965
J. Phys. Chem. B XXXX, XXX, XXX−XXX

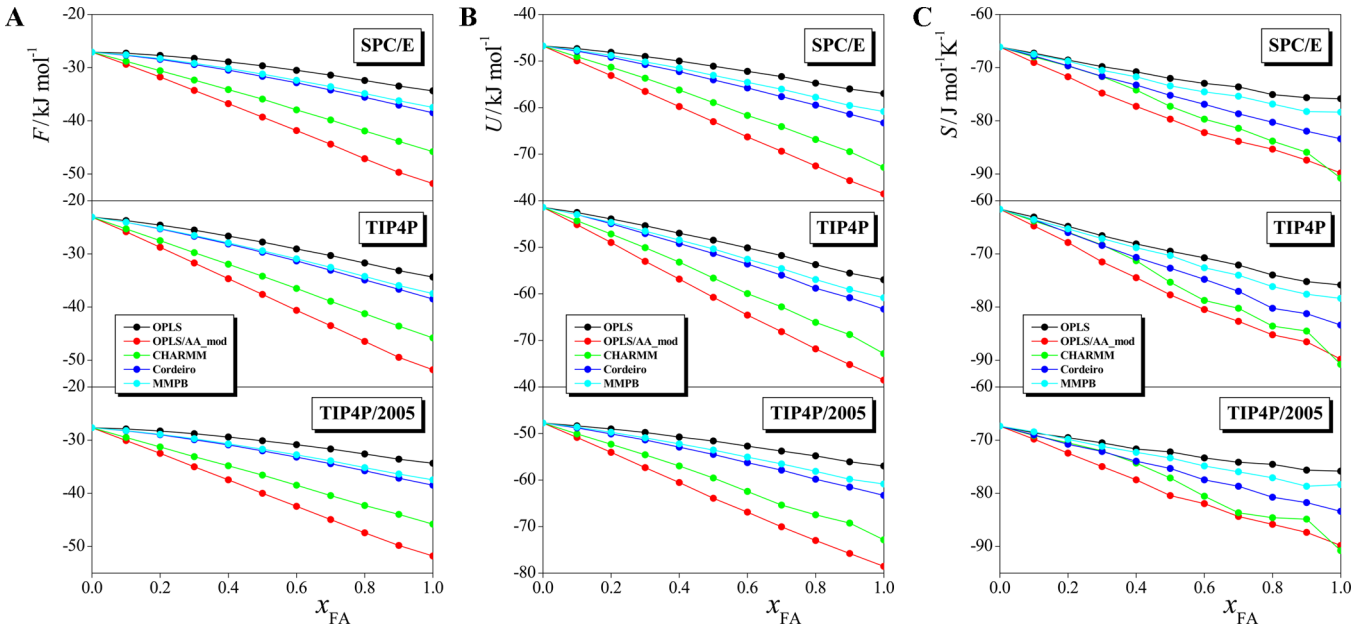

Figure 3. (a) Helmholtz free energy, (b) energy, and (c) entropy of mixtures of the SPC/E (top panel), TIP4P (middle panel), and TIP4P/2005 (bottom panel) water, and OPLS (black), OPLS/AA_mod (red), CHARMM (green), Cordeiro (dark blue), and MMPB (light blue) formamide models of various compositions with respect to the ideal gas state. The data obtained by thermodynamic integration are shown by full circles; the lines connecting the symbols only serve as guides to the eye. Error bars are typically below ±0.2 kJ/mol and ±1 J/(mol K).

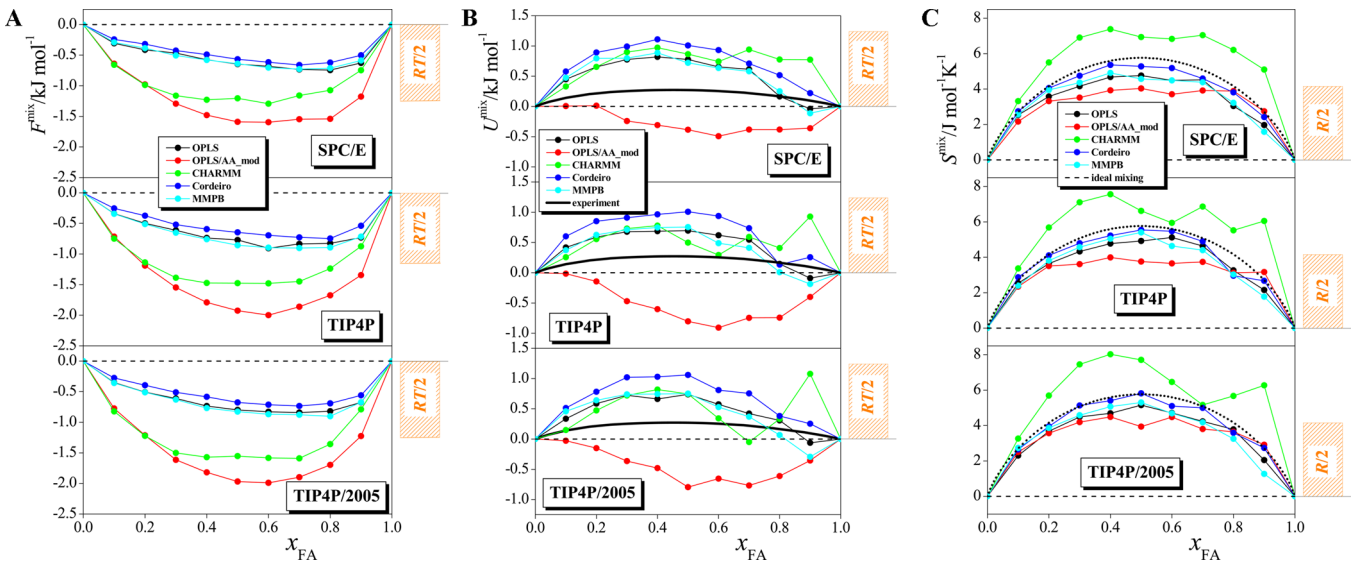

Figure 4. (a) Helmholtz free energy of mixing, (b) energy of mixing, and (c) entropy of mixing of the SPC/E (top panel), TIP4P (middle panel), and TIP4P/2005 (bottom panel) models of water with the OPLS (black), OPLS/AA_mod (red), CHARMM (green), Cordeiro (dark blue), and MMPB (light blue) models of formamide. Error bars are typically below ±0.2 kJ/mol and ±1 J/(mol K). The calculated data are shown by full circles; the lines connecting the symbols only serve as guides to the eye. Zero value is indicated by dashed line, experimental data of the energy of mixing (ref 12, 13) is shown by a thick line in panel (b), the entropy of ideal mixing is shown by dotted line in panel (c). The average kinetic energy of the molecules along one degree of freedom of $RT/2$ (for the Helmholtz free energy and energy of mixing) and $R/2$ (for the entropy of mixing) is also shown for reference by orange bars.

free energy of mixing with water is simply the consequence of the ideal term in the entropy of mixing. It should finally be noted that both the energy and entropy of mixing values turned out to be very close to the term corresponding to ideal mixing (i.e., 0 for U^{mix} and $-R\,[x_{FA}\ln x_{FA} + (1 - x_{FA})\ln(1 - x_{FA})]$ for S^{mix}) for every model combination and at every composition, confirming our previous suggestion, based on the nearly linear dependence the Helmholtz free energy, energy, and entropy of the liquid phase on x_{FA} (see Figure 3) that the mixing of these to compounds is nearly ideal.

As it has been emphasized previously, a negative value of F^{mix} is a necessary but not sufficient condition of miscibility; the two components are fully miscible with each other if and only if the value of the D parameter, defined in eq 1, is positive in the entire composition range. To determine the $D(x_{FA})$ data for the different model combinations, we fitted the Margules equation:[59]

DOI: 10.1021/acs.jpcb.7b04965
J. Phys. Chem. B XXXX, XXX, XXX−XXX

$$F^{ex}/RT = x_{FA}(1 - x_{FA})[A_{12}x_{FA} + A_{21}(1 - x_{FA}) - (C_{12}x_{FA} + C_{21}(1 - x_{FA}))x_{FA}(1 - x_{FA}) + Bx_{FA}^2(1 - x_{FA})^2] \quad (12)$$

where A_{12}, A_{21}, C_{12}, C_{21}, and B are the Margules parameters, to the calculated $F^{ex}(x_{FA})$ data, and calculated the second derivative of this fitted function. The quality of the Margules fit is illustrated in the inset of Figure 5 for the mixtures of the OPLS/AA_mod model of formamide with the SPC/E and TIP4P/2005 water models.

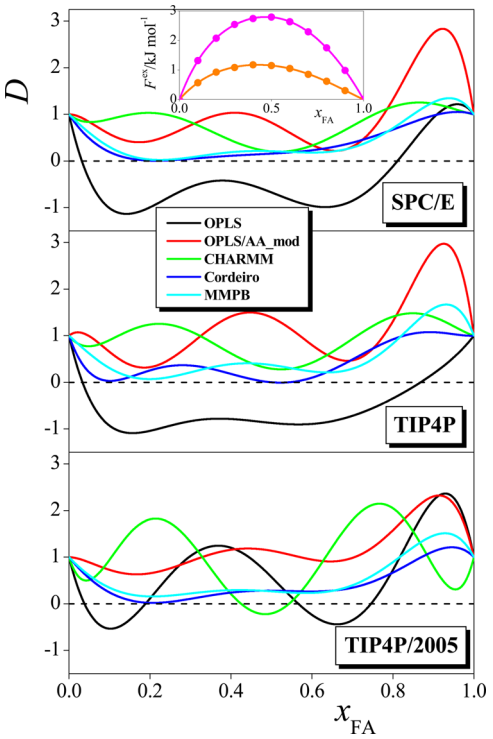

Figure 5. Composition dependence of the parameter D, defined by eq 1, in mixtures of the SPC/E (top panel), TIP4P (middle panel), and TIP4P/2005 (bottom panel) water, and OPLS (black), OPLS/AA_mod (red), CHARMM (green), Cordeiro (dark blue), and MMPB (light blue) formamide models. Estimated uncertainty of the data is below ±0.1. The inset shows the calculated F^{ex} data (full circles), together with their Margules fit (eq 12, solid curves) for mixtures of the OPLS/AA_mod model of formamide with the SPC/E (orange) and TIP4P/2005 (magenta) water models.

The $D(x_{FA})$ curves obtained with the different model combinations considered are shown in Figure 5. As is seen from the figure, the curves obtained with the combinations of the OPLS model of formamide with the SPC/E and TIP4P water models drop below zero in a wide composition range, extending from the x_{FA} value of 0.02−0.03 to about 0.8−0.85, indicating that these model combinations are largely immiscible with each other. The OPLS and TIP4P/2005 models show two narrow immiscibility gaps, in the x_{FA} ranges of about 0.04−0.2 and 0.55−0.75. Further, the $D(x_{FA})$ curves obtained using the Cordeiro and MMPB formamide models in combination with any of the three water models considered goes very close to zero, the former dropping always D = 0.05, while the latter below D = 0.15 at certain compositions. Although the $D(x_{FA})$ curve is positive in the entire composition range in the case of these six model combinations, its minimum is close to, or it is even below the estimated uncertainty of the D data of about 0.1, thus, immiscibility of some of these model combinations might occur in a narrow composition range. Further, full miscibility of these model combinations might also depend on the details of the simulation (e.g., long-range correction, etc.).

On the other hand, the D values obtained using the OPLS/AA_mod formamide model with any of the three water models considered remains safely above zero in the entire composition range, indicating that the OPLS/AA_mod model is indeed fully miscible with all these three water models. On the other hand, as it has been pointed out previously, these model combinations are qualitatively incompatible with existing experimental data[12,13] in respect to the energy of mixing, as they correspond to negative rather than positive energy of mixing values in the entire composition range (see Figure 4b).

Finally, the $D(x_{FA})$ curves obtained with the CHARMM model of formamide exhibit a clear minimum around the equimolar composition. The value of this minimum is around 0.2 when the SPC/E, and 0.28 when the TIP4P water model is used, but drops clearly below zero in combination with the TIP4P/2005 water model. Thus, the CHARMM and TIP4P/2005 models exhibit a narrow miscibility gap in the x_{FA} range of about 0.4−0.55, while the CHARMM model of formamide is fully miscible with both the SPC/E and TIP4P water models. Further, as seen from Figure 4b, these model combinations are also qualitatively compatible with the experimental data[12,13] concerning the sign of the energy of mixing. Considering also the fact that the $D(x_{FA})$ curve remains farther above zero when the TIP4P rather than the SPC/E water model is used, we recommend the use of the combination of the CHARMM model of formamide and TIP4P model of water when water−formamide mixtures are simulated.

Finally, it should be noted that whenever the value of D is found to drop below zero, it remains relatively small in magnitude, never going below about −1. This means that the thermodynamic driving force of the immiscibility of the corresponding model combinations is rather small. Therefore, in simulations of the bulk liquid phase, when demixing is also suppressed by the use of periodic boundary conditions, the occurrence of a visible phase separation might require much longer simulations than what is usually done.[60] However, if the liquid mixture is in contact with an anisotropic object, such as in the presence of the liquid−vapor interface, phase separation occurs rather quickly.

SUMMARY AND CONCLUSIONS

In this article we have studied the thermodynamic changes that occur upon mixing water and formamide as well as their miscibility in computer simulation using the combination of five formamide and three water models. The Helmholtz free energy, energy, and entropy of mixing of these model pairs have been calculated along an appropriately chosen thermodynamic cycle using the method of thermodynamic integration. To evaluate the performance of the various model combinations, we used the well-known fact that these compounds are fully miscible with each other,[1] and the experimental values of their energy of mixing in the entire composition range.[12,13]

The results have revealed that the mixing of the two molecules is nearly ideal, as the values of both the energy and the entropy of mixing have turned out to be close to the ideal term in the entire composition range. The free energy of mixing has been found to be always negative, indicating that the mixtures are always more stable than the two neat components.

DOI: 10.1021/acs.jpcb.7b04965
J. Phys. Chem. B XXXX, XXX, XXX−XXX

However, concerning the origin of this negative free energy of mixing, different models of formamide have shown different behavior. Thus, in the case of the OPLS/AA_mod model, this is mainly of energetic origin (as here the energy of mixing is always negative, while the entropy of mixing is clearly smaller than the value corresponding to ideal mixing), while in the case of the other four formamide models considered, it is clearly of entropic origin (as the energy of mixing is positive). Existing experimental data supports this latter behavior.[12,13]

The OPLS model of formamide has been found to exhibit miscibility gaps with all the three water models considered, while the model combinations involving the Cordeiro or MMPB formamide models very closely approach the miscibility limit at a certain composition, and hence full miscibility in these cases might also depend on the exact conditions under which the simulations are performed. Finally, the CHARMM model of formamide has shown limited miscibility with the TIP4P/2005 model, but full miscibility with the SPC/E and TIP4P models of water. Since the latter of these two model combinations remains farther from the miscibility limit than the former one, the present results allow us to recommend the use of the combination of the CHARMM model of formamide and TIP4P model of water in simulations of water−formamide mixtures.

AUTHOR INFORMATION

Corresponding Author

*E-mail: jedlovszky.pal@uni-eszterhazy.hu.

ORCID

Abdenacer Idrissi: 0000-0002-6924-6434

Milán Szőri: 0000-0003-4895-0999

Pál Jedlovszky: 0000-0001-9304-435X

Notes

The authors declare no competing financial interest.

ACKNOWLEDGMENTS

The authors acknowledge financial support from the NKFIH Foundation, Hungary (project number 119732) from the Hungarian-French TéT (PHC Balaton) program under project Nos. 36402ND (France) and TÉT_15-1-2016-0029 (Hungary). M.Sz. is a Bolyai János Research Scholar of the Hungarian Academy of Sciences (BO/00113/15/7). This research was supported by the European Union and the Hungarian State, cofinanced by the European Regional Development Fund in the framework of the GINOP-2.3.4-15-2016-00004 project, aimed to promote the cooperation between the higher education and the industry.

REFERENCES

(1) Höhn, A. Formamide. In *Kirk-Othmer Encyclopedia of Chemical Technology*; Kroschwitz, J. I., Ed.; Wiley: New York, 2000.

(2) Jorgensen, W. L.; Swenson, C. J. Optimized Intermolecular Potential Functions for Amides and Peptides. Structure and Properties of Liquid Amides. *J. Am. Chem. Soc.* **1985**, *107*, 569−578.

(3) Wohlfarth, C. *Landolt-Börnstein: Numerical Data and Functional Relationships in Science and Technology, Group 4, Vol. 6, Static Dielectric Constants of Pure Liquids and Binary Liquid Mixtures*; Springer: Berlin, 1991.

(4) Geiger, A.; Stillinger, F. H.; Rahman, A. Aspects of the Percolation Process for Hydrogen-Bond Networks in Water. *J. Chem. Phys.* **1979**, *70*, 4185−4193.

(5) Stanley, H. E.; Teixeira, J. Interpretation of the Unusual Behavior of H_2O and D_2O at Low Temperatures. Test of a Percolation Model. *J. Chem. Phys.* **1980**, *73*, 3404−3422.

(6) Tsuchida, E. Ab Initio Molecular-Dynamics Study of Liquid Formamide. *J. Chem. Phys.* **2004**, *121*, 4740−4746.

(7) Bakó, I.; Megyes, T.; Bálint, Sz.; Chihaia, V.; Bellissent-Funel, M. C.; Krienke, H.; Kopf, A.; Suh, S. H. Hydrogen Bonded Network Properties in Liquid Formamide. *J. Chem. Phys.* **2010**, *132*, 014506−1−7.

(8) Elola, M. D.; Ladanyi, B. M. Computational Study of Structural and Dynamical Properties of Formamide-Water Mixtures. *J. Chem. Phys.* **2006**, *125*, 184506−1−13.

(9) Jadżyn, J.; Świergiel, J. On Similarity of Hydrogen-Bonded Networks in Liquid Formamide and Water As Revealed in the Static Dielectric Studies. *Phys. Chem. Chem. Phys.* **2012**, *14*, 3170−3175.

(10) Elola, M. D.; Ladanyi, B. M. Intermolecular Polarizability Dynamics of Aqueous Formamide Liquid Mixtures Studied by Molecular Dynamics Simulations. *J. Chem. Phys.* **2007**, *126*, 084504−1−13.

(11) Puhovski, Y. P.; Rode, B. M. Molecular Dynamics Simulations of Aqueous Formamide Solution. 2. Dynamics of Solvent Molecules. *J. Chem. Phys.* **1995**, *102*, 2920−2927.

(12) Zaichikov, A. M.; Golubinskii, O. E. Enthalpy of Mixing of Water with Some Primer and Secunder Amides. *Zh. Fiz. Khim.* **1996**, *70*, 1175−1179 (in Russian).

(13) Zaichikov, A. M. Termochemical Study of the Ternary System Water-Formamide-Dimethylacetamide. *Russ. J. Gen. Chem.* **2001**, *71*, 162−167.

(14) Zoranić, L.; Mazighi, R.; Sokolić, F.; Perera, A. Concentration Fluctuations and Microheterogeneity in Aqueous Amide Mixtures. *J. Chem. Phys.* **2009**, *130*, 124315−1−12.

(15) Considine, D. M.; Considine, G. D. Formamide. In *Van Nostrand's Scientific Encyclopedia*; Considine, D. M., Ed.; Wiley: New York, 2005.

(16) Ma, X.; Yu, J. Formamide as the Plasticizer for Thermoplastic Starch. *J. Appl. Polym. Sci.* **2004**, *93*, 1769−1773.

(17) Howard, P. H. *Handbook of Environmental Fate and Exposure Data for Organic Chemicals*; CRC Press: Boca Raton, 1993; Vol. *IV*.

(18) Marechal, Y. Infrared Spectra of a Poorly Known Species: Water. 3. *J. Phys. Chem.* **1993**, *97*, 2846−2850.

(19) Tolosa, S.; Hidalgo, A.; Sansón, J. A. Thermodynamic, Structural, and Dynamic Study of the N-H···O═C Hydrogen Bond Association in Aqueous Solution. *Chem. Phys.* **2000**, *255*, 73−84.

(20) Sagarik, K. P.; Ahlrichs, R. A Test Particle Model Potential for Formamide and Molecular Dynamics Simulations of the Liquid. *J. Chem. Phys.* **1987**, *86*, 5117−5126.

(21) Thompson, H. B.; LaPlanche, L. A. Electric Moments of N,N-Disubstituted Amides. *J. Phys. Chem.* **1963**, *67*, 2230−2231.

(22) Puhovski, Y. P.; Rode, B. M. Structure and Dynamics of Liquid Formamide. *Chem. Phys.* **1995**, *190*, 61−82.

(23) Šponer, J. E.; Šponer, J.; Nováková, O.; Brabec, V.; Šedo, O.; Zdráhal, Z.; Costanzo, G.; Pino, S.; Saladino, R.; Di Mauro, E. Emergence of the First Catalytic Oligonucleotides in a Formamide-Based Origin Scenario. *Chem. - Eur. J.* **2016**, *22*, 3572−3586.

(24) Menor-Salván, C.; Marín-Yaseli, M. R. Prebiotic Chemistry in Eutectic Solutions at the Water−Ice Matrix. *Chem. Soc. Rev.* **2012**, *41*, 5404−5415.

(25) Szőri, M.; Jójárt, B.; Izsák, R.; Szőri, K.; Csizmadia, I. G.; Viskolcz, B. Chemical Evolution of Biomolecule Building Blocks. Can Thermodynamics Explain the Accumulation of Glycine in the Prebiotic Ocean? *Phys. Chem. Chem. Phys.* **2011**, *13*, 7449−7458.

(26) Essex, J. W.; Jorgensen, W. L. Dielectric Constants of Formamide and Dimethylformamide Via Computer Simulation. *J. Phys. Chem.* **1995**, *99*, 17956−17962.

(27) Cordeiro, J. M. M. C-H···O and N-H···O Hydrogen Bonds in Liquid Amides Investigated by Monte Carlo Simulation. *Int. J. Quantum Chem.* **1997**, *65*, 709−717.

(28) Pérez de la Luz, A.; Méndez-Maldonado, G. A.; Núñez-Rojas, E.; Bresme, F.; Alejandre, J. A New Force Field of Formamide and the

DOI: 10.1021/acs.jpcb.7b04965
J. Phys. Chem. B XXXX, XXX, XXX−XXX

(29) Macchiagodena, M.; Mancini, G.; Pagliai, M.; Barone, V. Accurate Prediction of Bulk Properties in Hydrogen Bonded Liquids: Amides As Case Studies. *Phys. Chem. Chem. Phys.* **2016**, *18*, 25342−25354.
(30) Puhovski, Y. P.; Rode, B. M. Molecular Dynamics Simulations of Aqueous Formamide Solution. 1. Structure of Binary Mixtures. *J. Phys. Chem.* **1995**, *99*, 1566−1576.
(31) Cordeiro, M. A. M.; Santana, W. P.; Cusinato, R.; Cordeiro, J. M. M. Monte Carlo Investigation of Intermolecular Interactions in Water-Amide Mixtures. *J. Mol. Struct.: THEOCHEM* **2006**, *759*, 159−164.
(32) Biswas, S.; Mallik, B. S. Aqueous Solvation of an Amide Molecule from First Principle Simulations: Structure, Hydrogen Bond Dynamics and Spectral Signature. *J. Mol. Liq.* **2015**, *212*, 941−946.
(33) Bakó, I.; Oláh, J.; Lábas, A.; Bálint, Sz.; Pusztai, L.; Bellissent Funel, M. C. Water-Formamide Mixtures: Topology of the Hydrogen-Bonded Network. *J. Mol. Liq.* **2017**, *228*, 25−31.
(34) Jedlovszky, P.; Idrissi, A.; Jancsó, G. Can Existing Models Qualitatively Describe the Mixing Behavior of Acetone with Water? *J. Chem. Phys.* **2009**, *130*, 124516−1−7.
(35) Pinke, A.; Jedlovszky, P. Modeling of Mixing Acetone and Water: How Can Their Full Miscibility Be Reproduced in Computer Simulations? *J. Phys. Chem. B* **2012**, *116*, 5977−5984.
(36) Darvas, M.; Jedlovszky, P.; Jancsó, G. Free Energy of Mixing of Pyridine and Its Methyl-Substituted Derivatives with Water, As Seen from Computer Simulations. *J. Phys. Chem. B* **2009**, *113*, 7615−7620.
(37) Mezei, M.; Beveridge, D. L. Free Energy Simulations. *Ann. N. Y. Acad. Sci.* **1986**, *482*, 1−23.
(38) Leach, A. R. *Molecular Modelling*; Longman: Singapore, 1996.
(39) Idrissi, A.; Vyalov, I.; Kiselev, M.; Jedlovszky, P. Assessment of the Potential Models of Acetone/CO_2 and Ethanol/CO_2 Mixtures by Computer Simulation and Thermodynamic Integration in Liquid and Supercritical States. *Phys. Chem. Chem. Phys.* **2011**, *13*, 16272−16281.
(40) Idrissi, A.; Polok, K.; Barj, M.; Marekha, B.; Kiselev, M.; Jedlovszky, P. Free Energy of Mixing of Acetone and Methanol − a Computer Simulation Investigation. *J. Phys. Chem. B* **2013**, *117*, 16157−16164.
(41) Idrissi, A.; Marekha, B.; Barj, M.; Jedlovszky, P. Thermodynamics of Mixing Water with Dimethyl Sulfoxide, As Seen from Computer Simulations. *J. Phys. Chem. B* **2014**, *118*, 8724−8733.
(42) Smith, J. M.; Van Ness, H. C.; Abbott, M. M. *Introduction to Chemical Engineering Thermodynamics*; McGraw Hill: Boston, 2001.
(43) Mezei, M.; Swaminathan, S.; Beveridge, D. L. Ab Initio Calculation of the Free Energy of Liquid Water. *J. Am. Chem. Soc.* **1978**, *100*, 3255−3256.
(44) Mezei, M. Direct Calculation of the Excess Free Energy of the Dense Lennard-Jones Fluid. *Mol. Simul.* **1989**, *2*, 201−207.
(45) Mezei, M. Polynomial Path for the Calculation of Liquid State Free Energies from Computer Simulations Tested on Liquid Water. *J. Comput. Chem.* **1992**, *13*, 651−656.
(46) Mináry, P.; Jedlovszky, P.; Mezei, M.; Turi, L. A Comprehensive Liquid Simulation Study of Neat Formic Acid. *J. Phys. Chem. B* **2000**, *104*, 8287−8294.
(47) Jedlovszky, P.; Pártay, L. B.; Bartók, A. P.; Voloshin, V. P.; Medvedev, N. N.; Garberoglio, G.; Vallauri, R. Structural and Thermodynamic Properties of Different Phases of Supercooled Liquid Water. *J. Chem. Phys.* **2008**, *128*, 244503−1−12.
(48) Davis, P. J.; Polonsky, I. Numerical Interpolation, Differentiation and Integrtion. In *Handbook of Mathematical Functions with Formulas, Graphs, and Mathematical Tables*; Abramowitz, M., Stegun, I. A., Eds.; National Bureau of Standards: Washington, D. C., 1972; pp 875−924.
(49) García, B.; Alcalde, R.; Leal, J. M.; Matos, J. S. Solute-Solvent Interactions in Amide-Water Mixed Solvents. *J. Phys. Chem. B* **1997**, *101*, 7991−7997.
(50) Mezei, M. *MMC: Monte Carlo Program for Simulation of Molecular Assemblies*. http://inka.mssm.edu/~mezei/mmc.
(51) Barker, J. A.; Watts, R. O. Monte Carlo Studies of the Dielectric Properties of Water-Like Models. *Mol. Phys.* **1973**, *26*, 789−792.
(52) Neumann, M. The Dielectric Constant of Water. Computer Simulations with the MCY Potential. *J. Chem. Phys.* **1985**, *82*, 5663−5672.
(53) Allen, M. P.; Tildesley, D. J. *Computer Simulation of Liquids*; Clarendon Press: Oxford, 1987.
(54) Jorgensen, W. L.; Maxwell, D. S.; Tirado-Rives, J. Development and Testing of the OPLS All-Atom Force Field on Conformational Energetics and Properties of Organic Liquids. *J. Am. Chem. Soc.* **1996**, *118*, 11225−11236.
(55) Bjelkmar, P.; Larsson, P.; Cuendet, M. A.; Hess, B.; Lindahl, E. Implementation of the CHARMM Force Field in GROMACS: Analysis of Protein Stability Effects from Correction Maps, Virtual Interaction Sites, and Water Models. *J. Chem. Theory Comput.* **2010**, *6*, 459−466.
(56) Berendsen, H. J. C.; Grigera, J. R.; Straatsma, T. The Missing Term in Effective Pair Potentials. *J. Phys. Chem.* **1987**, *91*, 6269−6271.
(57) Jorgensen, W. L.; Chandrasekhar, J.; Madura, J. D.; Impey, R.; Klein, M. L. Comparison of Simple Potential Functions for Simulating Liquid Water. *J. Chem. Phys.* **1983**, *79*, 926−935.
(58) Abascal, J. L. F.; Vega, C. A General Purpose Model for the Condensed Phases of Water: TIP4P/2005. *J. Chem. Phys.* **2005**, *123*, 234505−1−12.
(59) Villamañán, M. A.; Van Ness, H. C. Excess Thermodynamic Properties for Water/Acetone. *J. Chem. Eng. Data* **1984**, *29*, 429−431.
(60) Perera, A.; Sokolić, F. Modeling Nonionic Aqueous Solutions: The Acetone-Water Mixture. *J. Chem. Phys.* **2004**, *121*, 11272−11282.

DOI: 10.1021/acs.jpcb.7b04965
J. Phys. Chem. B XXXX, XXX, XXX−XXX